



EFFECTS OF RADIATION AND MASS TRANSFER ON MAGNETOHYDRODYNAMIC CONVECTION FLOW PAST AN IMPULSIVELY STARTED VERTICAL PLATE INUNDATED IN A POROUS MEDIUM WITH VISCOUS DISSIPATION

Sadashiv P. Dahake^{#1}, A.V. Dubewar^{*2}

^{#1} Department of Mathematics, Shah & Anchor Kutchhi Engineering College
Mumbai- 400088, India

^{#2} Department of Mathematics, Datta Meghe College of Engineering
Navi Mumbai- 400708, India

ABSTRACT

An investigation study is carried out to obtain the effects of radiation on unsteady free convection heat and mass transfer of viscous incompressible flow through the saturated porous medium with viscous dissipation. The flow is considered under the influence of magnetic field applied normal to the flow. The equations of continuity, linear momentum, energy and diffusion, which govern the flow field, are solved by employing the Crank-Nicolson's implicit method. The behavior of the velocity, temperature, concentration, skin-friction, Nusselt number and Sherwood number has been examined for variations in the interaction of flow parameters.

Key words: *finite difference, free convection, radiation, saturated porous medium, viscous dissipation*

1. Introduction:

Combined heat and mass transfer and radiation problems are of importance in numerous processes and have, therefore, received remarkable amount of attention in recent years such as in the industrial furnace systems, turbines, nuclear power plants, forest fire dynamics, astrophysical flows, oil reservoir engineering, and fire spread in buildings. A detailed review of the subject of flow in porous media, including exhaustive list of references, was recently

done by Nield and Bejan [1], Ingham and Pop [2], Vafai [3] The problem of free convection boundary layer flow past a vertical plate is of fundamental interest to many technological applications in the modern industry. Many authors have contributed with some important theoretical, analytical results to this problem when the fluid properties are constant. Soundalgekar [4] investigated unsteady free convection flow along vertical porous plate with different boundary conditions and viscous dissipation effect. Vajravelu [5] studied natural convection flow along a heated semi-infinite vertical plate with internal heat generation. Cookey *et al.* [6] studied influence of viscous dissipation and radiation on unsteady MHD free convective flow past an infinite heated vertical plate in a porous medium with time dependent suction. Chamkha [7] discussed unsteady MHD convective heat and mass transfer past a semi-infinite vertical permeable moving plate with heat generation. Ahmed [8] studied effects of unsteady free convective MHD flow through a porous medium bounded by an infinite vertical porous plate. Sharma and Singh (16) discussed unsteady MHD free convective flow and heat transfer along a vertical porous plate with variable suction and internal heat generation. Sharma *et al.* [9] analyzed the heat and mass transfer effects on unsteady MHD free convective flow along a vertical porous plate with internal heat generation and variable suction. **A V. Dubewar and V. M. Soundalgekar** [10] studied the mass transfer effects on free convection flow past an infinite vertical porous plate This paper investigates the effects of radiation and mass transfer on magneto hydrodynamic convection flow past an impulsively started vertical plate embedded in a porous medium with viscous dissipation and the mathematical model of the problem is developed. The numerical procedure is outlined whilst discussions and results are presented with the help of graphs.

2. Mathematical Analysis:

We consider an unsteady laminar natural convection flow of a viscous incompressible, dissipative, electrically conducting and viscous radiating fluid past an impulsively started infinite vertical plate in the presence of transverse magnetic field. We made the following assumptions to develop the flow model.

- i. The fluid is assumed to be gray, absorbing-emitting but non-scattering.
- ii. The \bar{x} -axis is chosen along the plate in the vertical upward direction while the \bar{y} -axis is taken perpendicular to the plate at the leading edge.
- iii. The origin of \bar{x} -axis is taken to be at the leading edge of the plate.
- iv. The gravitational field g is acting downward.

- v. At time $\bar{t} = 0$, it is assumed that the plate and the fluid are at the same ambient temperature \bar{T}_∞ species concentration \bar{C}_∞ .
- vi. A uniformly transverse magnetic field is applied in the direction of flow. It is also assumed that the interaction of the induced magnetic field with the flow is considered to be negligible in comparison to the interaction of the applied magnetic field with the flow.
- vii. When $\bar{t} > 0$, the temperature of the plate and the species concentration are maintained at \bar{T}_w and \bar{C}_w respectively.
- viii. When $\bar{t} = 0$, the temperature of the plate and the fluid are considered to be at the temperatures \bar{T}_∞ and \bar{C}_∞ respectively.
- ix. A uniform magnetic field is applied in the normal direction of flow.
- x. The fluid properties are considered to be constant except the body forces terms (in momentum equation) which are approximated by Boussinesq equation.

Assuming Boussinesq's approximation for an incompressible fluid model, the governing equations of the flow for an optically thin medium are

$$\frac{\partial \bar{u}}{\partial x} + \frac{\partial \bar{v}}{\partial y} = 0 \quad \text{---- (1)}$$

$$\frac{\partial \bar{u}}{\partial t} + \bar{u} \frac{\partial \bar{u}}{\partial x} + \bar{v} \frac{\partial \bar{u}}{\partial y} = \nu \frac{\partial^2 \bar{u}}{\partial y^2} + g\beta_r(\bar{T} - \bar{T}_\infty) + g\beta_c(\bar{C} - \bar{C}_\infty) - \frac{\sigma B_o^2}{\rho} \bar{u} - \frac{\nu}{\kappa} \bar{u} - \frac{b}{\kappa} \bar{u}^2 \quad \text{---- (2)}$$

$$\frac{\partial \bar{T}}{\partial t} + \bar{u} \frac{\partial \bar{T}}{\partial x} + \bar{v} \frac{\partial \bar{T}}{\partial y} = \alpha \frac{\partial^2 \bar{T}}{\partial y^2} + \frac{\nu}{C_p} \left(\frac{\partial \bar{u}}{\partial y} \right)^2 - \frac{1}{\rho C_p} \frac{\partial q_r}{\partial y} \quad \text{---- (3)}$$

$$\frac{\partial \bar{C}}{\partial t} + \bar{u} \frac{\partial \bar{C}}{\partial x} + \bar{v} \frac{\partial \bar{C}}{\partial y} = D \frac{\partial^2 \bar{C}}{\partial y^2} \quad \text{---- (4)}$$

The corresponding initial and boundary conditions are

$$\left. \begin{aligned} &\bar{u} = 0, \bar{v} = 0, \bar{T} = \bar{T}_\infty, \bar{C} = \bar{C}_\infty \quad \text{for } \bar{t} \leq 0 \\ &\text{for } \bar{t} > 0, \bar{u} = \bar{u}_0, \bar{v} = 0, \bar{T}_w = \bar{T}_\infty, \bar{C}_w = \bar{C}_\infty \quad \text{at } \bar{y} = 0 \\ &\text{for } \bar{t} > 0, \bar{u} = 0, \bar{T}_w = \bar{T}_\infty, \bar{C}_w = \bar{C}_\infty \quad \text{at } \bar{x} = 0 \\ &\text{for } \bar{t} > 0, \bar{u} \rightarrow 0, \bar{T}_w \rightarrow \bar{T}_\infty, \bar{C}_w \rightarrow \bar{C}_\infty \quad \text{as } \bar{y} \rightarrow \infty \end{aligned} \right\} \quad \text{---- (5)}$$

By using the Rosseland diffusion flux is used and defined following

$$q_r = -\frac{4\sigma^*}{3K_e} \frac{\partial \bar{T}^4}{\partial y} \quad \text{---- (6)}$$

where σ is the Stephen Boltzmann constant and K_e is the mean absorption coefficient. It should be noted that by using the Rosseland approximation, the present analysis is limited to optically thick fluids. If the temperature differences within the flow are sufficiently small,

then equation (6) can be linearized by expanding \bar{T}^4 into the Taylor series about T_∞ , which after neglecting higher order terms takes the form

$$\bar{T}^4 \cong 4\bar{T}_\infty^3\bar{T} - 3\bar{T}_\infty^4 \quad \text{---- (7)}$$

Using equation (7), the energy equation (3) becomes

$$\frac{\partial \bar{T}}{\partial t} + \bar{u} \frac{\partial \bar{T}}{\partial x} + \bar{v} \frac{\partial \bar{T}}{\partial y} = \alpha \frac{\partial^2 \bar{T}}{\partial y^2} + \frac{\nu}{C_p} \left(\frac{\partial \bar{u}}{\partial y} \right)^2 + \frac{16\sigma \bar{T}_\infty^3}{\rho C_p Ke} \frac{\partial^2 \bar{T}}{\partial y^2} \quad \text{---- (8)}$$

In order to write the governing equations and the boundary conditions in dimensionless form, the following non-dimensional quantities are introduced

$$\left. \begin{aligned} x &= \frac{\bar{x}\bar{u}_0}{\nu}, & y &= \frac{\bar{y}\bar{u}_0}{\nu} \\ u &= \frac{\bar{u}}{\bar{u}_0}, & v &= \frac{\bar{v}}{\bar{u}_0}, & t &= \frac{\bar{u}_0^2}{\nu} \\ Ec &= \frac{\bar{u}_0^2}{C_p(\bar{T}_w - \bar{T}_\infty)} \\ T &= \frac{(\bar{T} - \bar{T}_\infty)}{(\bar{T}_w - \bar{T}_\infty)}, \\ C &= \frac{(\bar{C} - \bar{C}_\infty)}{(\bar{C}_w - \bar{C}_\infty)} \end{aligned} \right\} \text{---- (9a)}$$

$$\left. \begin{aligned} Pr &= \frac{\nu}{\alpha}, & Re &= \frac{L\bar{u}_0}{\nu}, & Sc &= \frac{\nu}{D} \\ Gr &= \frac{g \beta \nu (\bar{T}_w - \bar{T}_\infty)}{\bar{u}_0^3} \\ Gm &= \frac{g \nu \beta (\bar{C}_w - \bar{C}_\infty)}{\bar{u}_0^3}, \\ Da &= \frac{K}{L^2}, & Fs &= \frac{b}{L} \\ N &= \frac{k'k}{4\sigma \bar{T}_\infty^3}, & M &= \frac{\sigma B_0^2 \nu}{\rho \bar{u}_0^2} \end{aligned} \right\} \text{----- (9b)}$$

On substitution of Equations (9a) and (9b) into Equations (1), (2), (4) and (8) the following governing equations are obtained in non-dimensional form

$$\frac{\partial u}{\partial x} + \frac{\partial u}{\partial y} = 0 \quad \text{---- (10)}$$

$$\frac{\partial u}{\partial t} + u \frac{\partial u}{\partial x} + v \frac{\partial u}{\partial y} = GrT + GmC + \frac{\partial^2 u}{\partial y^2} - MU - \frac{U}{Re^2 Da} - \frac{FsU^2}{Da Re} \quad \text{---- (11)}$$

$$\frac{\partial T}{\partial t} + u \frac{\partial T}{\partial x} + v \frac{\partial T}{\partial y} = \frac{1}{Pr} \left(1 + \frac{4}{3N} \right) \frac{\partial^2 T}{\partial y^2} + Ec \left(\frac{\partial u}{\partial y} \right)^2 \quad \text{---- (12)}$$

$$\frac{\partial C}{\partial t} + u \frac{\partial C}{\partial x} + v \frac{\partial C}{\partial y} = \frac{1}{Sc} \frac{\partial^2 C}{\partial y^2} \quad \text{---- (13)}$$

As following in [11] the Darcy-Forchheimer inertia term F_s is added to velocity equation. The corresponding initial and boundary conditions for velocity, temperature and concentration fields in non-dimensional form are

$$\left. \begin{aligned} u &= 0, v = 0, T = 0, C = 0 \text{ for } t \leq 0 \\ \text{for } t > 0, u &= 1, v = 0, T = 1, C = 1 \text{ at } y = 0 \\ \text{for } t > 0, u &= 0, T = 0, C = 0 \text{ at } x = 0 \\ \text{for } t > 0, u &\rightarrow 0, T \rightarrow 0, C_w \rightarrow 0 \text{ as } y \rightarrow \infty \end{aligned} \right\} \text{---- (14)}$$

Now it is important to calculate the physical quantities of primary interest, which are the local shear stress, local surface heat flux and Sherwood number.

Dimensionless local wall shear stress or skin-friction is obtained as,

$$\tau_x = -\left(\frac{\partial y}{\partial y}\right)_{y=0} \text{ ----- (15)}$$

Dimensionless local surface heat flux or Nusselt number is obtained as

$$Nu_x = -\left(\frac{\partial T}{\partial y}\right)_{y=0} \text{ ---- (16)}$$

Dimensionless the local Sherwood number is obtained

$$Sh_x = -x\left(\frac{\partial C}{\partial y}\right)_{y=0} \text{ ---- (17)}$$

3. Method of solution:

Equations (10)-(13) are coupled nonlinear partial differential equations are solved using boundary and initial conditions (14). All the same, exact or approximate solutions are not possible. Therefore we solve these equations by Crank-Nicolson implicit finite difference method for numerical solution. The equivalent finite difference scheme of Equations (10) - (13) as given in [11, 12] is adopted. The finite difference equations corresponding to (10)-(13) are:

$$\frac{u_{i,j}^{k+1} - u_{i-1,j}^{k+1} + u_{i,j}^k - u_{i-1,j}^k + u_{i,j-1}^{k+1} - u_{i-1,j-1}^{k+1} + u_{i,j-1}^k - u_{i-1,j-1}^k}{4(\Delta x)} + \frac{v_{i,j}^{k+1} - v_{i,j-1}^{k+1} + v_{i,j}^k - v_{i,j-1}^k}{2(\Delta y)} = 0 \text{ ----- (18)}$$

$$\frac{u_{i,j}^{k+1} - u_{i,j}^k}{\Delta t} + u_{i,j}^k \frac{u_{i,j}^{k+1} - u_{i,j-1}^{k+1} + u_{i,j}^k - u_{i,j-1}^k}{2(\Delta x)} + v_{i,j}^k \frac{u_{i,j+1}^{k+1} - u_{i,j-1}^{k+1} + u_{i,j+1}^k - u_{i,j-1}^k}{4(\Delta y)} =$$

$$Gr \frac{T_{i,j}^{k+1} + T_{i,j}^k}{2} + Gm \frac{C_{i,j}^{k+1} + C_{i,j}^k}{2} + \frac{u_{i,j-1}^{k+1} - 2u_{i,j}^{k+1} + u_{i,j+1}^{k+1} + u_{i,j-1}^k - 2u_{i,j}^k + u_{i,j+1}^k}{2(\Delta y)^2} -$$

$$\frac{1}{Re^2 Da} \frac{u_{i,j}^{k+1} + u_{i,j}^k}{2} - \frac{Fs}{Da Re} \frac{u_{i,j}^{k+1} + u_{i,j}^k}{2} - M \frac{u_{i,j}^{k+1} + u_{i,j}^k}{2} \text{ ---- (19)}$$

$$\frac{T_{i,j}^{k+1} + T_{i,j}^k}{\Delta t} + u_{i,j}^k \frac{T_{i,j}^{k+1} - T_{i-1,j}^{k+1} + T_{i,j}^k - T_{i-1,j}^k}{2(\Delta x)} + v_{i,j}^k \frac{T_{i,j+1}^{k+1} - T_{i,j-1}^{k+1} + T_{i,j+1}^k - T_{i,j-1}^k}{4(\Delta y)} =$$

$$\frac{1}{Pr} \left(1 + \frac{4}{3N}\right) \frac{T_{i,j-1}^{k+1} - 2T_{i,j}^{k+1} + T_{i,j+1}^{k+1} + T_{i,j-1}^k - 2T_{i,j}^k + T_{i,j+1}^k}{2(\Delta y)^2} + Ec \left(\frac{u_{i,j+1}^k - u_{i,j}^k}{2\Delta y}\right)^2 \text{ ---- (20)}$$

$$\frac{C_{i,j}^{k+1} - C_{i,j}^k}{\Delta t} + u_{i,j}^k \frac{C_{i,j}^{k+1} - C_{i-1,j}^{k+1} + C_{i,j}^k - C_{i-1,j}^k}{2(\Delta x)} + v_{i,j}^k \frac{C_{i,j+1}^{k+1} - C_{i,j-1}^{k+1} + C_{i,j+1}^k - C_{i,j-1}^k}{4(\Delta y)} =$$

$$\frac{1}{Sc} \frac{C_{i,j-1}^{k+1} - 2C_{i,j}^{k+1} + C_{i,j+1}^{k+1} + C_{i,j-1}^k - 2C_{i,j}^k + C_{i,j+1}^k}{2(\Delta y)^2} \quad \text{---- (21)}$$

The computational domain is considered as a rectangle with sides $x_{\max} = 1$ and $y_{\max} = 5.3$, where y_{\max} corresponds to $y \rightarrow \infty$ which was very well outside the momentum, energy and species boundary layers. The approximation of $u(x, y, t)$ and $v(x, y, t)$ at the grid point $(i\Delta x, j\Delta y, k\Delta t)$ are denoted by $u_{i,j}^k$ and $v_{i,j}^k$ respectively where Δx is the grid size in x -direction, Δy is the grid size in y -direction and Δt is the increment in time t . The mesh sizes are considered to be $\Delta x = 0.1$ in x -direction, $\Delta y = 0.25$ in y -direction and $\Delta t = 0.01$ in k -direction. By using initial conditions at $t=0$, the values of u , v , C and T are calculated at all grid points. The values of u , v , C and T at next time level $(k + 1)$ are calculated using the known values at previous time level (k) . Hence, the finite difference equation forms a tridiagonal system of equations at each internal node point on a particular i th level which is solved with the help of Matlab code.

Thus, we compute the values of C and T at each nodal point for a particular i at $(k + 1)$ th time level and the results were used in u at $(k + 1)$ th time level. The values of v are also calculated at every nodal point explicitly on a particular i -level at $(k + 1)$ th time level. In this way, the values of u , v , C and T are known at all grid point at time level $(k + 1)$ in the region. The process is repeated several times for various i -level until the required time is reached. In order to test the accuracy of the results, we have compared the velocity profile against y for various values of Species, Grashof number, Schmidt number, thermal Grashof number and Conduction-radiation parameter with the Crank-Nicolson calculation of Prasad *et al.* [12]. Velocity profiles represented by Fig.1 shows the effect of Gr , Gm and Sc numbers and N for $t = 0.75$ and $x = 1$. It is observed that the present results are in good agreement with that of available solution of Prasad *et al.* [12].

4. Results and discussions:

In order to get an insight into the problem, we present the results of numerical computations of velocity, temperature and concentration for different values of Nusselt number, Sherwood number magnetic field parameter M , the conduction-radiation heat parameter N and time t . Pr physically relates the relative thickness of hydrodynamic and thermal boundary layers while Sc relates the relative thickness of hydrodynamic and concentration boundary layers. Unless otherwise stated the values for parameters are assumed to be

$Gr=20, Gm = 20, Da = 0.1, Fs = 0.1, Re = 1, Pr = 0.71$ (air), $Sc = 0.6, N = 3.0, M = 1.0, Ec = 0.001$ which are related about optically thick boundary layers.

The effects of Gr , Gm and M on the dimensionless velocity profile against y - co-ordinate are shown in [Fig. 2](#). An increase in Gr / Gm causes a raise in the velocity profiles, an increase in Grashof number push up the buoyancy force. The increase shows a steep rise in the velocity near the wall and goes down towards zero. An increase magnetic parameter, M decreases the velocity profile which asserts the fact that the presence of magnetic field depresses the force on the free convective flow.

The influence of viscous dissipation parameter i.e., Eckert number Ec on the dimensionless velocity profile of the fluid are presented in [Fig. 3 -4](#) respectively. From these figures, it is seen that presence of magnetic field on electrically conducting fluid results in the rise Lorentz force which reverses and retards the motion of a fluid. Also it is observed that with increase in values of Ec increases the velocity profile. The dissipation function quickens energy in the fluid motion as a result the buoyancy force increases.

[Fig. 5-6](#) investigates the effects of varying values of magnetic field on the temperature and species concentration profiles. Temperature increases marginally with the increasing value of magnetic field parameter for the species concentration and temperature.

The effect of N and Darcy number, Da on the temperature profile is presented in [Fig. 7-8](#). An increase in N causes a significant decrease in the temperature values from the greatest value at the wall $y=0$ across the boundary layer to the free stream. Thus, greater value of N relates to smaller radiation flux and the minimum temperature are observed for $N=5$ in [fig.7](#). The rate of energy transport to the fluid is reduced by Thermal radiation. In [fig.8](#), as Darcy number Da increases, a rise in temperature profile is observed. This rise temperature profile means that conduction heat transfer is more prevalent than convection heat transfer.

[Fig. 9 -10](#) shows the effects of Sc on the velocity and temperature profiles. It may be noted that the velocity and temperature diminishes due to a rise in Sc . [Fig.10](#) shows that temperature reduces sharply with an increase in Schmidt number, which entails a reduction in diffusivity of the species. The concentration profile comes down from its maximum concentration to zero in the free stream.

Fig. 11-12 shows the effects of Darcy-Forchheimer inertia term F_s on the velocity profile. As F_s decreases, we observe great increase in the velocity profile. In the momentum equation, the quadratic term is directly proportional to F_s . This suggests that, as F_s rises from 0.2 to 20, we observe a steep reduction in velocity component. Fig. 11 shows the effects of the thermal Grashof number and the conduction radiation parameter N on the concentration profile. As Gr rises from 0.4 to 75 in Fig. 12, we observed a much decrease in the species concentration in the boundary layer flow.

Fig. 13-15 delineates the variation of the local skin friction, local Nusselt number and the local Sherwood number with stream wise distance x for different values of the Eckert number. In Fig. 13, it is observed that local skin friction increases due to increase in Ec . In Fig. 14, the local Nusselt number for different values of Ec is depicted. Nusselt number is defined as the ratio of convective heat transfer coefficient to conductive heat transfer coefficient. It can be seen that Nusselt number Nu diminishes with greater viscous dissipative heat. That is heat transfer rates are reduced by an increase in Ec i.e. dissipation parameter. Sherwood number represents the ratio between mass transfer by convection and mass transfer by diffusion. It is noticed in Fig. 15 that the Sherwood number, Sh increments because of the presence of higher viscous heat dissipation.

5. Conclusions:

In this work we have analyzed thermal radiation effects on unsteady MHD flow past an impulsively started vertical plate embedded in porous medium in presence of viscous dissipation. From present numerical study the following conclusions can be drawn:

1. Increasing temperature and concentration in presence of magnetic field, decelerates the velocity.
2. An increase in the conduction- radiation parameter (N) causes reduction in the velocity profile while a rise in the dissipation function induces a considerable rise in velocity.
3. Increase in the Prandtl number, Schmidt number, species Grashof number, thermal Grashof number and the conduction-radiation parameter causes the temperature to reduce, while a rise in the Darcy number Da causes a rise in temperature along and normal to the wall.
4. Increase in Forchheimer number F_s reduces the velocity profile. Shear stress was found to increase with a rise in Ec at the wall while the Local Nusselt number

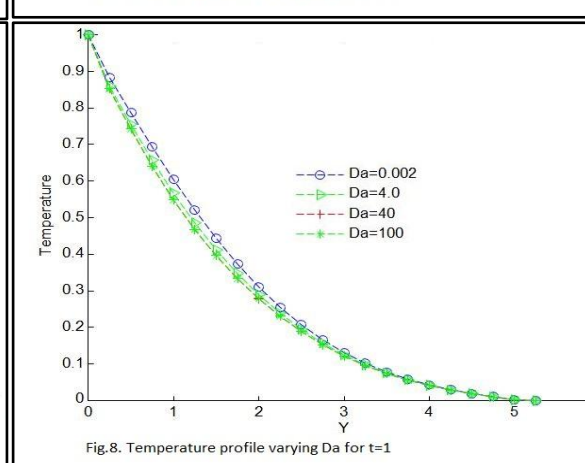
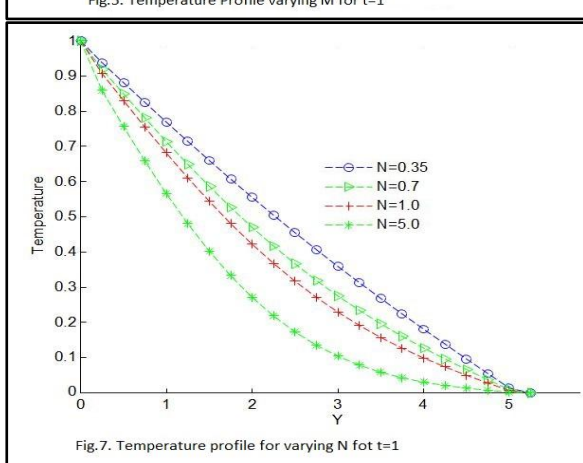
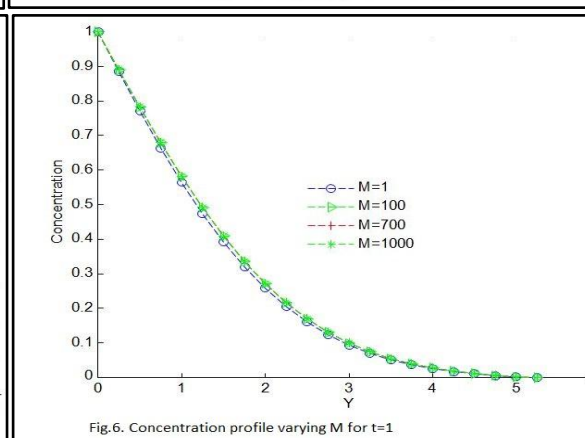
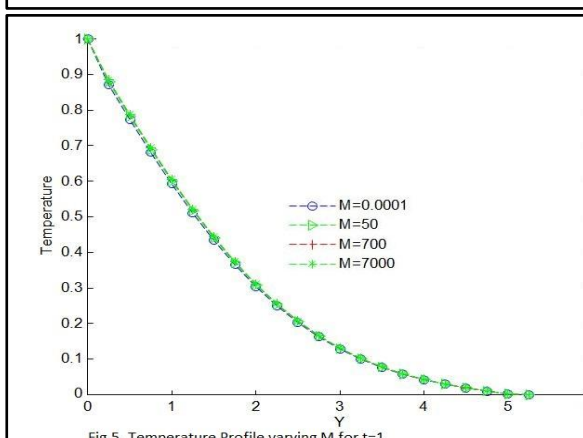
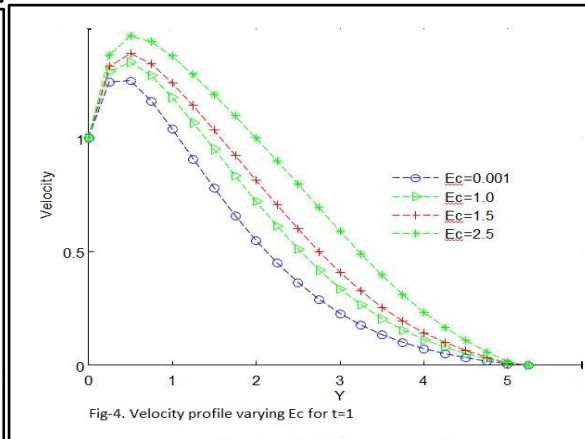
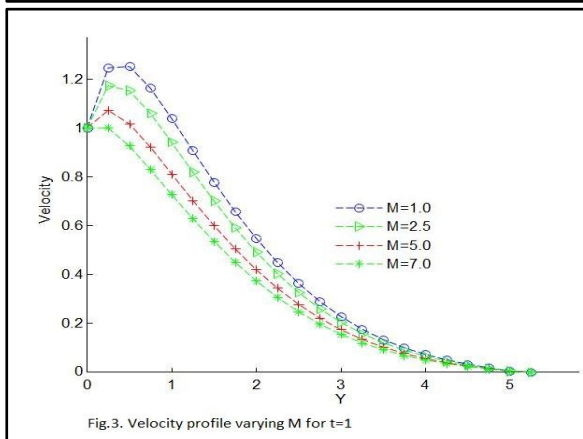
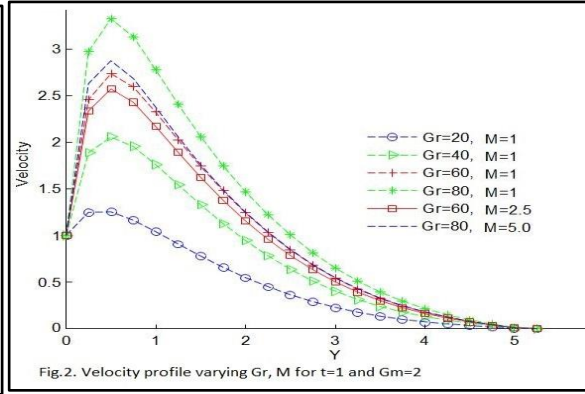
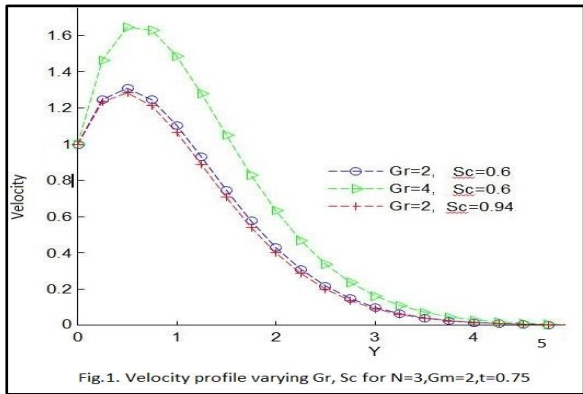
increased with reduction in Ec .

5. Sherwood number increases with an increase in Ec .

References:

- [1] Nield, D.A., Bejan, A., *Convection in Porous Media*, 3rd ed., Springer, New York, 2006.
- [2] Ingham, D.B., Pop, I., *Transport Phenomena in Porous Media*, Elsevier, Oxford, 2005.
- [3] Vafai, K., (ed.), *Handbook of Porous Media*, 2nd ed., Taylor & Francis, New York, 2005
- [4] Soundalgekar V. M., unsteady free convection flow along vertical porous plate with different boundary conditions and viscous dissipation effect. *Int. J. Heat Mass Transfer*, 15, (1971), pp.1253-1261.
- [5] Vajravelu K., Natural convection flow along a heated semi-infinite vertical plate with internal heat generation. *Acta Mech.*, 34, (1979), pp.153-159.
- [6] Cooney C., Ogulu A., Omubo-Pepple V. B., Influence of viscous dissipation and radiation on unsteady MHD free convective flow past an infinite heated vertical plate in a porous medium with time dependent suction. , *Int. J. Heat Mass Transfer*, 46, (2003), pp. 2305-2311.
- [7] Chamkha A.J., Unsteady MHD convective heat and mass transfer past a semi-infinite vertical permeable moving plate with heat generation., *Int. J. Sci. Engg.*, 13 (4), (2010), pp. 359-364.
- [8] Ahmed S., Effects of unsteady free convective MHD flow through a porous medium bounded by an infinite vertical porous plate. *Bull. Cal. Math. Soc.*, 90, (2007), pp.507-522.
- [9] Sharma P. R., Dadkeech I. K. and Gurminder Singh., The heat and mass transfer effects on unsteady MHD free convective flow along a vertical porous plate with internal heat generation and variable suction. *Int. J. of Math Archive*, 3(5), (2012), pp. 2163-2172.
- [10] A.V. Dubewar, V. M. Soundalgekar, Mass transfer effects on free convection flow past an infinite vertical porous plate, *Int. J. of Applied Mechanics and Engg*, 10(4), (2005), pp.605-615.

- [11] A.J. Chamka, H.S. Takhar, O.A. Beg, Numerical modeling of Darcy-Brinkman Forchheimer magnetohydrodynamic mixed convection flow in a porous medium with transpiration and viscous heating, *Int. J. of Fluid Mechanics Research*, 29(1), (2002), pp.1-26.
- [12] Suneetha Sangapatnam, Bhaskar Reddy, Ramchandra Prasad, Radiation and mass transfer effects on MHD free convection flow past an impulsively started isothermal vertical plate with dissipation. *Thermal science: vol. 13(2)* (2009), pp. 171-181
- [13] V. Ramachandra Prasad a, N. Bhaskar Reddy, R. Muthucumaraswamy, Radiation and mass transfer effects on two-dimensional flow past an impulsively started infinite vertical plate. *International Journal of Thermal Sciences* 46 (2007) pp. 1251–1258



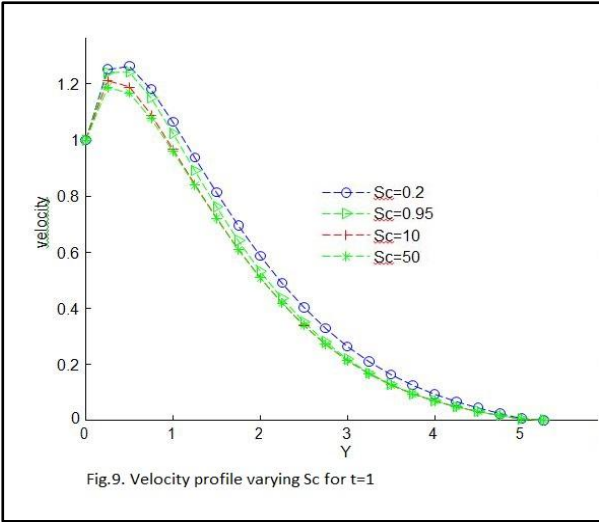


Fig.9. Velocity profile varying Sc for $t=1$

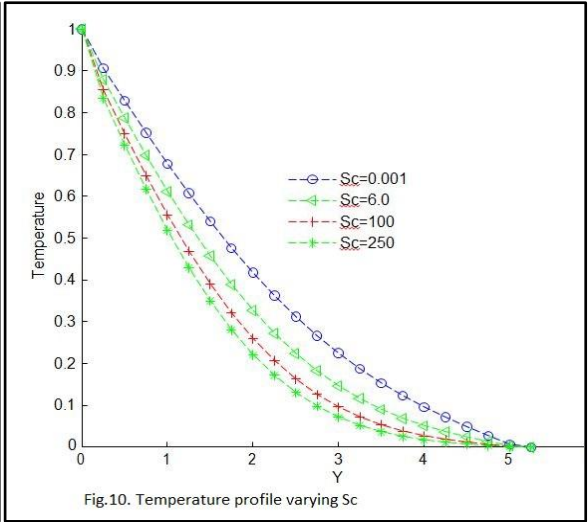


Fig.10. Temperature profile varying Sc

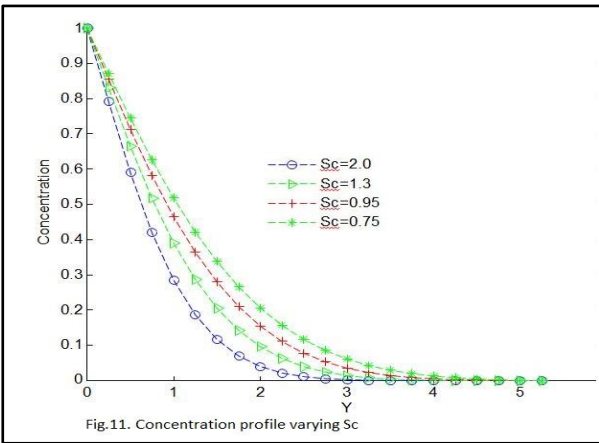


Fig.11. Concentration profile varying Sc

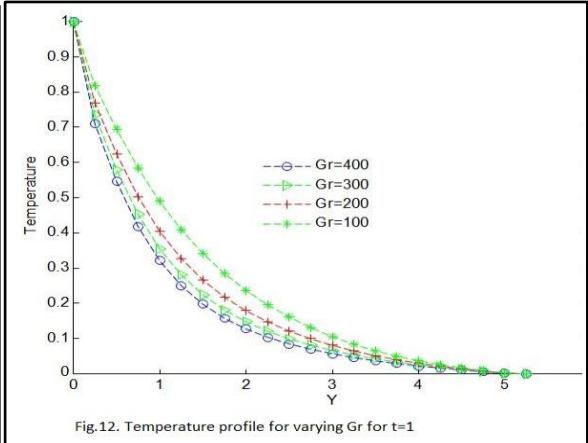


Fig.12. Temperature profile for varying Gr for $t=1$

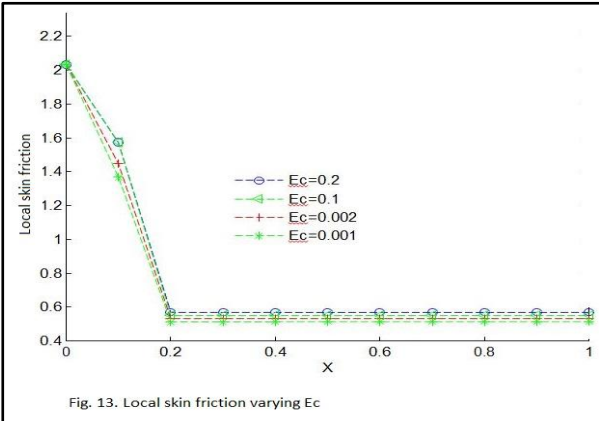


Fig.13. Local skin friction varying Ec

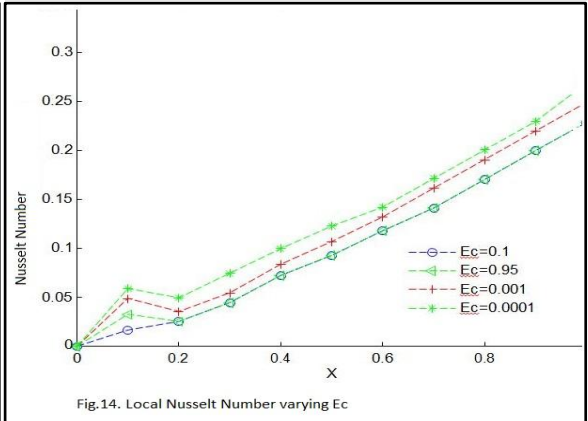


Fig.14. Local Nusselt Number varying Ec

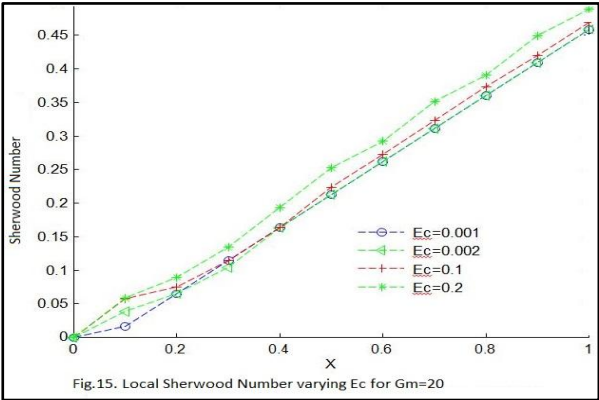


Fig.15. Local Sherwood Number varying Ec for $Gm=20$